Direct Observation of Josephson Capacitance

M. A. Sillanpää,[1] T. Lehtinen,[1] A. Paila,[1] Yu. Makhlin,[1,2] L. Roschier,[1] and P. J. Hakonen[1]

[1]*Low Temperature Laboratory, Helsinki University of Technology, FIN-02015 HUT, Finland*

[2]*Landau Institute for Theoretical Physics, 119334 Moscow, Russia*

(Received 20 April 2005; published 11 November 2005)

The effective capacitance has been measured in the split Cooper-pair box (CPB) over its phase-gate bias plane. Our low-frequency reactive measurement scheme allows us to probe purely the capacitive susceptibility due to the CPB band structure. The data are quantitatively explained using parameters determined independently by spectroscopic means. In addition, we show in practice that the method offers an efficient way to do nondemolition readout of the CPB quantum state.

DOI: 10.1103/PhysRevLett.95.206806 PACS numbers: 85.25.Cp, 85.35.Gv

Energy can be stored into Josephson junctions (JJ) according to $E = -E_J \cos(\varphi)$, where φ is the phase difference across the junction, and the Josephson energy E_J is related to the junction critical current I_C through $I_C = 2eE_J/\hbar$. By using the Josephson equations, this energy storing property translates into the well-known fact that a single classical JJ behaves as a parametric inductance $L_J = \hbar/(2eI_C)$ for small values of φ.

Since the early 1980s, it has become understood that φ itself can behave as a quantum-mechanical degree of freedom [1]. In mesoscopic JJs, this is typically associated with the competition between the Josephson and Coulomb effects at a very low temperature. These fundamental phenomena take place if charge on the junction is localized by a large resistance $R > R_Q = h/(4e^2)$ [2], as well as in the Cooper-pair box (CPB), or the single-Cooper-pair transistor (SCPT), whose quantum coherence is often considered macroscopic [3].

In the first theoretical landmark papers [4,5] on quantum properties of φ it was already noticed that due to localization of charge Q, the energy of a the JJ system is similar to that of a nonlinear capacitance. In spite of the importance of the phenomenon especially in CPB or SCPT in the promising field of superconducting qubits [6,7], direct experimental verification of the Josephson capacitance has been lacking, likely due to challenges posed by measuring small reactances, or by the extreme sensitivity to noise.

In this Letter, we present the first such direct experiment [8], where we determine the Josephson capacitance in the Cooper-pair box. Related experiments have recently been performed by Wallraff *et al.* [9], but in their case the key role is played by the transitions between levels of a coupled system where the band gap between the ground state and first excited state of the CPB, $E_1 - E_0 = \Delta E$, is nearly at resonance with an oscillator of angular frequency ω_0. Thus, detuning fully dominates over the Josephson capacitance which can be clearly observed in our experiments where we study directly the reactive response of the lowest band E_0 at a frequency $\omega_0 \ll \Delta E/\hbar$. We determine the experimental parameters independently using spectroscopy, and demonstrate a simple way to perform a nondestructive measurement of the CPB state using purely the CPB Josephson capacitance.

An SCPT (Fig. 1) consists of a mesoscopic island (total capacitance $C = C_1 + C_2 + C_g$), two JJs, and of a nearby gate electrode used to polarize the island with the (reduced) gate charge $n_g = C_g V_g/e$. The island has the charging energy $E_C = e^2/(2C)$, and the junctions have the generally unequal Josephson energies $E_J(1 \pm d)$, where the asymmetry is given by d. The SCPT Hamiltonian is then $E_C(\hat{n} - n_g)^2 - 2E_J \cos(\varphi/2) \times \cos(\hat{\theta}) + 2dE_J \sin(\varphi/2)\sin(\hat{\theta}) - C_g V_g^2/2$. Here, the number $\hat{n}$ of extra electron charges on the island is conjugate to $\hat{\theta}/2$, where $\hat{\theta}$ is the superconducting phase on the island [10]. The SCPT is thus equivalent to a CPB (single JJ and a capacitance in series with a gate voltage source) but with a Josephson energy tunable by $\varphi = 2\pi\Phi/\Phi_0$, where $\Phi_0 = h/(2e)$ is the quantum of magnetic flux.

If $d = 0$ and $E_J/E_C \ll 1$ the ground and excited state energies are $(n_g = 0 \ldots 2)$: $E_{0,1} = E_C(n_g^2 - 2n_g + 2) \mp \sqrt{[E_J \cos(\varphi/2)]^2 + [2E_C(1 - n_g)]^2} - C_g V_g^2/2$, with a large

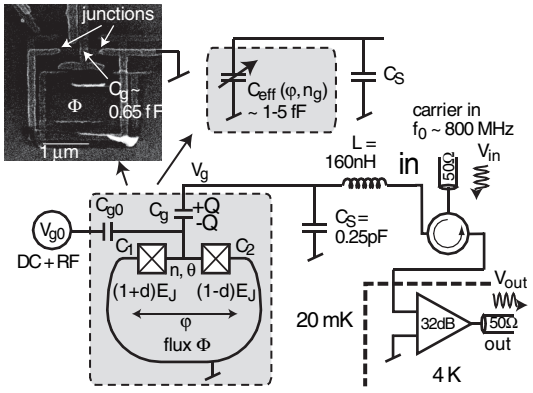

FIG. 1. Schematic view of the experiment. The resonant frequency of the LC circuit (made using lumped elements) is tuned by the effective capacitance C_{eff} of the Cooper-pair box shown in the SEM image. For details, see text.

gap to higher levels. For a general E_J/E_C, we compute the bands numerically in the charge state basis.

The effective ''Josephson'' capacitance of the CPB can be related to the curvature of band k, similar to the effective mass of an electron in a crystal:

$$C_{\text{eff}}^{k} = -\frac{\partial^2 E_k(\varphi, n_g)}{\partial V_g^2} = -\frac{C_g^2}{e^2}\frac{\partial^2 E_k(\varphi, n_g)}{\partial n_g^2}. \quad (1)$$

Usually, the system effective capacitance is obtained from a Lagrangian or Hamiltonian as $\partial^2\mathcal{L}/\partial V_g^2 = (\partial^2 H/\partial Q^2)^{-1}$, without the minus sign. In Eq. (1), however, E_k's are, more precisely, the eigenvalues of the *Routhian* $\mathcal{H} = \dot{\theta}\partial_{\dot{\theta}}\mathcal{L} - \mathcal{L}$ [11], which serves as a Hamiltonian for the n, θ degree of freedom but as *minus* Lagrangian for the phase $\alpha \equiv \frac{e}{\hbar}\int V_g dt$ and $V_g \propto \dot{\alpha}$, thus leading to Eq. (1).

Using the analytic formulas for $E_{0,1}$ in the limit $E_J/E_C \ll 1$ we get

$$C_{\text{eff}}^{(0,1)} = C_g - \frac{2C_g^2 E_C}{e^2} \times\left(1 \mp \frac{E_C E_J^2(1+\cos\varphi)}{[4E_C^2(n_g-1)^2 + \frac{1}{2}E_J^2(1+\cos\varphi)]^{3/2}}\right), \quad (2)$$

which reduces to the classical geometric capacitance $[1/C_g + 1/(C_1 + C_2)]^{-1}$ in the limit of vanishingly small E_J, except where Cooper-pair tunneling is degenerate [12]. Numerically evaluated graphs of $C_{\text{eff}}^{(0,1)}$ for a general E_J/E_C can be found in Ref. [13].

Our experimental scheme is illustrated in Fig. 1. We perform low-dissipation microwave reflection measurements [14,15] on a series LC resonator in which the box effective capacitance, Eq. (1), is a part of the total capacitance $C_S + C_{\text{eff}}^{k}$. The resonator is formed by a surface mount inductor of $L = 160$ nH. With a stray capacitance of $C_S = 250$ fF due to the fairly big lumped resonator, the resonant frequency is $f_0 = 800$ MHz and the quality factor $Q \simeq 16$ is limited by the external $Z_0 = 50\ \Omega$. When C_{eff}^{k} varies, the phase Θ of the reflected signal $V_{\text{out}} = \Gamma V_{\text{in}}$ changes, which is measured by the reflection coefficient $\Gamma = (Z - Z_0)/(Z + Z_0) = \Gamma_0 e^{i\Theta}$. Here, Z is the resonator impedance seen at the point labeled ''in'' in Fig. 1. In all the measurements, the probing signal V_{in} was continuously applied.

Since we are rather far from matching conditions, the reflection magnitude Γ_0 remains always close to 1. The variation in Θ due to modulation in C_{eff}^{k} is up to 40° in our measurements, corresponding to a shift of resonance frequency $\Delta f_0 \simeq 6$ MHz. In addition to bandpass filtering, we used two circulators at 20 mK.

As seen in Eq. (2), the modulation depth of C_{eff}^{k} is sensitive to C_g. Therefore, in order to faithfully demonstrate the Josephson capacitance in spite of the stray capacitance, we used a large $C_g > 0.5$ fF. It was made using an Al-AlO_x-Al overlay structure (see the image in Fig. 1), with a prolonged oxidization in 0.1 bar of O_2 for 15 min. Otherwise, our CPB circuits have been prepared using rather standard e-beam lithography. The tunnel junctions having both an area of 60 nm × 30 nm correspond to an average capacitance of ~0.17 fF each. The overlay gate has $C_g \simeq 0.7$ fF for an area of 180 nm × 120 nm.

The main benefit of our method comes from the fact that we work at a resonator (angular) frequency ω_0 much lower than the CPB level spacing ΔE. In Ref. [9] it is shown that ω_0 depends on the resonator—CPB (qubit) interaction because of two contributions. The frequency change is $\Delta\omega_0 = g^2/\delta$, where the detuning $\delta = \Delta E - \hbar\omega_0$, and the coupling coefficient g contains the curvature of energy bands. In general, both δ and the curvature depend on the (n_g, φ) point. Now, in our case everywhere $\Delta E \gg \hbar\omega_0$, $\delta \simeq \Delta E$, and hence $\Delta\omega_0 = g^2/\Delta E = C_{\text{eff}}\omega_0/(2C_S)$ has a contribution by only the second derivative, not by the detuning. Therefore, we can resolve the reactive response due to purely the bands of CPB, which has not been possible in previous experiments.

When doing microwave spectroscopy, we have to consider also the other side of the coin: ΔE increases due to interaction with the resonator by [16] $\varepsilon = \hbar(2Ng^2/\Delta E + g^2/\Delta E)$, where N is the number of quanta in the resonator. When driven by a gate amplitude V_g, the resonator energy is $E_R = V_g^2 C_S/2$. At a high excitation amplitude $n_g \simeq 1/2$ we would have $V_g \simeq e/(2C_g)$ and hence $N = E_R/(\hbar\omega_0) = e^2 C/(8C_g^2\hbar\omega_0) \sim 4 \times 10^3$ which would yield $\varepsilon \sim \Delta E$. The data shown in this Letter are, however, measured at a very low excitation of $n_g \sim 0.05$ which corresponds to $N \sim 40$ and $\varepsilon \sim 200$ MHz which is an insignificant contribution to ΔE.

Figure 2(a) displays the measured phase shift Θ as a function of the two external control knobs (in the following, n_g should be understood as being due to the control gate, $n_g = C_{g0}V_{g0}/e$). The results show full $2e$ periodicity as a function of n_g, checked by increasing temperature above the $2e - e$ crossover at ~300 mK, and a Φ_0 period with respect to Φ. The data were measured without any microwave excitation, and hence we expect to see effects due to the ground band C_{eff}^{0}. The corresponding theoretical picture, obtained using Eq. (1) and straightforward circuit formulas for Γ, is given in Fig. 2(b).

As a vital step to get convinced of the measured capacitance modulation versus the calculation, we carried out a detailed determination of the sample parameters independently of the capacitance modulation by using microwave spectroscopy (Fig. 3). To the weakly coupled control gate C_{g0} of the SCPT, we applied continuous-wave microwaves while slowly sweeping the CPB band gap ΔE with φ and n_g. Whenever the microwave energy matches the band gap, that is, $\hbar\omega_{\text{RF}} = \Delta E$, the CPB becomes resonantly excited. Since typically the Josephson corrections to the geometric capacitance are opposite in sign for the bands 0 and 1 [see Eq. (2)], band 1 would contribute an opposite phase shift signal. At resonance, we would then expect to see mixture of C_{eff}^{0} and C_{eff}^{1}, weighted by the state occupancies which

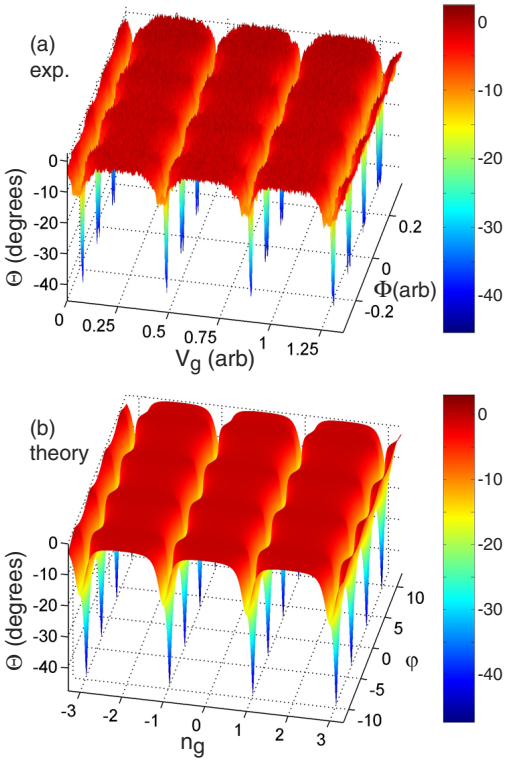

FIG. 2 (color online). (a) Phase shift Θ measured at a probing frequency 803 MHz $\sim f_0$, and (b) Θ calculated using Eq. (1) with the ground band $E_0(\varphi, n_g)$ evaluated numerically with parameters of Table I.

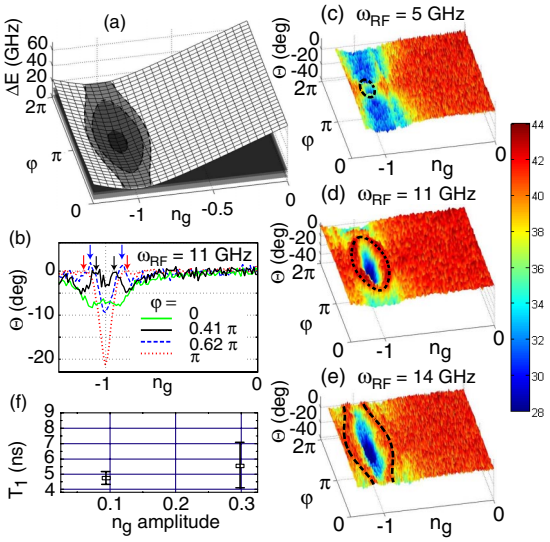

FIG. 3 (color online). (a) Illustration of the microwave spectroscopy used to map the SCPT band gap $\Delta E = E_1 - E_0$. The three horizontal planes which intersect the band gap correspond, from bottom to top, to the microwave energy $\hbar\omega_{\mathrm{RF}}$ used in (c)–(e), respectively. Whenever $\Delta E = \hbar\omega_{\mathrm{RF}}$ (dashed lines), the system experiences resonant absorption; (b) peaks of resonant absorption (arrows) in the measured phase shift at $\omega_{\mathrm{RF}} =$ 11 GHz; (c)–(e) spectroscopy data represented as surfaces in the φ, n_g plane. The resonance conditions shown in (a) are plotted on top of the data; (f) T_1 as a function of measurement strength at $\varphi = 0$, $n_g \sim 1$.

depend on the microwave amplitude. We calculate that a high enough amplitude sufficient to saturate the populations into a 50%–50% mixture would yield a ~3° resonance absorption peak in the measured Θ. The expectation is confirmed in Fig. 3(b), where the resonance peaks are displayed at a few values of φ (when $\varphi = 0$, microwave energy does not exceed the band gap, and for $\varphi = \pi$ the peak height is lower due to a smaller matrix element).

While slowly sweeping φ and n_g, the resonance conditions correspond to contours [see Fig. 3(a)], which appear as annular ridges in the experimental data of graphs [Fig. 3(c)–3(e)] around the minimum ΔE at $(n_g = -1, \varphi = \pi)$. Since the band gap is sensitive to E_J as well as to the E_J/E_C ratio, the resonance contours allow for an accurate determination of these parameters (Table I). For example, at $(n_g = -1, \varphi = 0)$, the band gap is $2E_J =$ 12.5 GHz, whereas at $(n_g = -1, \varphi = \pi)$ ΔE has the absolute minimum $2dE_J \simeq 3$ GHz which was barely exceeded by the microwave energy in Fig. 3(c).

Based on the surface area ~0.022 μm^2 of the overlay gate, we estimate $C_g \sim 0.5$–1 fF. The exact value was obtained by fitting to the modulation depth of C^0_{eff} [see Eq. (2)], yielding $C_g = 0.65$ fF, corresponding to a specific capacitance very reasonable to a thick oxide ~30 fF/μm^2.

Figure 4 illustrates the bare gate and flux modulations without microwave excitation in more detail, and shows the corresponding numerical calculations using the ground band. As expected, C_{eff} reduces to the geometric capacitance when Cooper-pair tunneling is blocked either by tuning the Josephson energy effectively to zero when φ is an odd multiple of π or by gate voltage. At the Coulomb resonance $n_g = \pm 1$, however, the Josephson capacitance is significant. In the special point $n_g = \pm 1$, $\varphi = \pm\pi$, the most pronounced effect is observed, now due to strong Cooper-pair fluctuations. The agreement between theory and experiment is good in Fig. 4 except around $n_g = \pm 1$ which we assign to intermittent poisoning by energetic quasiparticles [17]. An estimate using C_{eff} from Eq. (2), $\Theta = -2C_{\mathrm{eff}}\sqrt{L}/(C_S^{3/2}Z_0)$, falls to within 15% of the numerical results except around integer n_g.

Reactive measurements, either inductive or capacitive, can be employed for nondemolition readout for qubits [18] which means that $0 \leftrightarrow 1$ relaxation caused by the measurement is insignificant. An important advantage of our scheme is that since the probing gate swing has a frequency

TABLE I. Sample parameters determined by microwave spectroscopy. R_T is the series resistance of the two SCPT tunnel junctions (other parameters are defined in text and in Fig. 1).

E_J (K)	$E_C = \frac{e^2}{2C}$ (K)	E_J/E_C	R_T(kΩ)	C (fF)	d	C_g (fF)
0.30	0.83	0.36	55	1.1	0.22	0.65

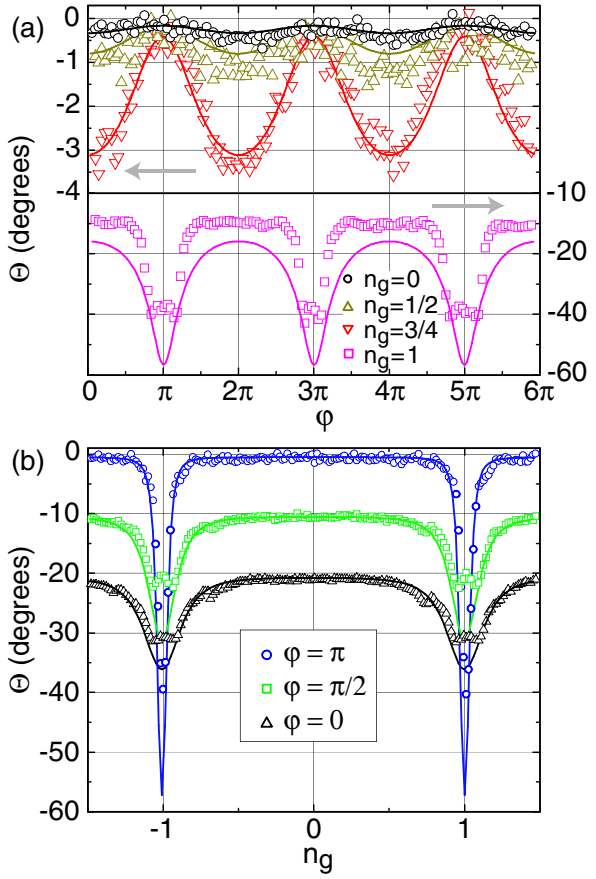

FIG. 4 (color online). Measured microwave phase shift Θ, (a) vs phase φ (note different scales in the two panels) and (b) vs gate charge n_g (curves for $\varphi = 0$ and $\pi/2$ have been shifted vertically for clarity by 20° and 10°, respectively). Solid lines are numerical calculations using Eq. (1) and sample parameters in Table I.

$f_0 \ll \Delta E/\hbar$, its contribution to spectral density at the qubit level spacing frequency is negligible. We measured the relaxation time T_1 using the technique of pulsed microwave excitation with variable repetition time $T_R =$ 1–200 ns, while keeping the measurement signal always on, as in Ref. [19]. The T_1 times were limited to about 7 ns by parasitic reactances in the somewhat uncontrolled high-frequency environment, causing noise from Z_0 to couple strongly due to a large coupling $\kappa = C_g/C \sim 1$. The result for T_1, however, did not depend on the measurement strength [Fig. 3(f)], which supports the nondemolition character of this scheme. By fabricating the resonator on chip it is straightforward to gain a full control of environment. Then, the impedance seen from the qubit gate $\mathrm{Re}[Z_g(\omega = \Delta E/\hbar)] \simeq 0.1$ mΩ, and a worst-case estimate yields $T_1 \approx \hbar R_K/\{4\pi\kappa^2\,\mathrm{Re}[Z_g(\Delta E/\hbar)]\Delta E\} \gg 1$ μs. For a dephasing time T_2 averaged over n_g, we measured $\sim$0.5 ns using Landau-Zener interferometry [20,21]. This T_2 time is on the same order as the spectroscopy linewidths in Fig. 3.

In conclusion, using the phase of strongly reflected microwave signals, we have experimentally verified the Josephson capacitance in a mesoscopic Josephson junction, i.e., the quantity dual to the Josephson inductance. Good agreement is achieved with the theory on the Josephson capacitance. Implications for nondestructive readout of quantum state of Cooper-pair box using the capacitive susceptibility are investigated.

We thank T. Heikkilä, F. Hekking, G. Johansson, M. Paalanen, and R. Schoelkopf for comments and useful criticism. This work was supported by the Academy of Finland and by the Vaisala Foundation of the Finnish Academy of Science and Letters.

[1] M. Tinkham, *Introduction to Superconductivity* (McGraw-Hill, New York, 1996).
[2] See, e.g., G. Schön and A. D. Zaikin, Phys. Rep. **198**, 237 (1990); J. S. Penttilä *et al.*, Phys. Rev. Lett. **82**, 1004 (1999).
[3] Y. Nakamura, Y. A. Pashkin, and J. S. Tsai, Nature (London) **398**, 786 (1999).
[4] A. Widom *et al.*, J. Low Temp. Phys. **57**, 651 (1984).
[5] D. V. Averin, A. B. Zorin, and K. Likharev, Sov. Phys. JETP **61**, 407 (1985); K. Likharev and A. Zorin, J. Low Temp. Phys. **59**, 347 (1985).
[6] D. V. Averin and C. Bruder, Phys. Rev. Lett. **91**, 057003 (2003).
[7] See, e.g., Yu. Makhlin, G. Schön, and A. Shnirman, Rev. Mod. Phys. **73**, 357 (2001).
[8] Capacitance of a nonequilibrium Cooper-pair box has been investigated recently: T. Duty *et al.*, this issue, Phys. Rev. Lett. **95**, 206807 (2005).
[9] A. Wallraff *et al.*, Nature (London) **431**, 162 (2004).
[10] The last term in the Hamiltonian typically does not influence the SCPT's dynamics and is typically omitted; it is important to keep it here since V_g becomes a dynamical variable.
[11] L. D. Landau and E. M. Lifshitz, *Mechanics* (Pergamon, Oxford, 1976).
[12] For single electron case, see M. Büttiker and C. A. Stafford, Phys. Rev. Lett. **76**, 495 (1996).
[13] M. A. Sillanpää, Ph.D. thesis, Helsinki University of Technology, 2005; http://lib.tkk.fi/Diss/2005/isbn9512275686/.
[14] M. A. Sillanpää, L. Roschier, and P. J. Hakonen, Phys. Rev. Lett. **93**, 066805 (2004).
[15] L. Roschier, M. Sillanpää, and P. Hakonen, Phys. Rev. B **71**, 024530 (2005).
[16] D. I. Schuster *et al.*, Phys. Rev. Lett. **94**, 123602 (2005).
[17] J. Aumentado, M. W. Keller, J. M. Martinis, and M. H. Devoret, Phys. Rev. Lett. **92**, 066802 (2004).
[18] A. Blais *et al.*, Phys. Rev. A **69**, 062320 (2004).
[19] T. Duty, D. Gunnarsson, K. Bladh, and P. Delsing, Phys. Rev. B **69**, 140503(R) (2004).
[20] A. V. Shytov, D. A. Ivanov, and M. V. Feigel'man, Eur. Phys. J. B **36**, 263 (2003).
[21] M. A. Sillanpää *et al.* (to be published).